

XMM-NEWTON SPECTROSCOPY OF THE HIGHLY POLARIZED AND LUMINOUS BROAD ABSORPTION LINE QUASAR CSO 755

O. SHEMMER,¹ W. N. BRANDT,¹ S. C. GALLAGHER,² C. VIGNALI,^{3,4} TH. BOLLER,⁵ G. CHARTAS,¹ AND A. COMASTRI⁴

Received 2005 July 11; accepted 2005 September 4

ABSTRACT

We present the results from *XMM-Newton* observations of the highly optically polarized broad absorption line quasar (BALQSO) CSO 755. By analyzing its X-ray spectrum with a total of ~ 3000 photons we find that this source has an X-ray continuum of ‘typical’ radio-quiet quasars, with a photon index of $\Gamma = 1.83^{+0.07}_{-0.06}$, and a rather flat (X-ray bright) intrinsic optical-to-X-ray spectral slope of $\alpha_{\text{ox}} = -1.51$. The source shows evidence for intrinsic absorption, and fitting the spectrum with a neutral-absorption model gives a column density of $N_{\text{H}} \sim 1.2 \times 10^{22} \text{ cm}^{-2}$; this is among the lowest X-ray columns measured for BALQSOs. We do not detect, with high significance, any other absorption features in the X-ray spectrum. Upper limits we place on the rest-frame equivalent width of a neutral (ionized) Fe K α line, $\leq 180 \text{ eV}$ ($\leq 120 \text{ eV}$), and on the Compton-reflection component parameter, $R \leq 0.2$, suggest that most of the X-rays from the source are directly observed rather than being scattered or reflected; this is also supported by the relatively flat intrinsic α_{ox} we measure. The possibility that most of the X-ray flux is scattered due to the high level of UV–optical polarization is ruled out. Considering data for 46 BALQSOs from the literature, including CSO 755, we have found that the UV–optical continuum polarization level of BALQSOs is not correlated with any of their X-ray properties. A lack of significant short- and long-term X-ray flux variations in the source may be attributed to a large black-hole mass in CSO 755. We note that another luminous BALQSO, PG 2112+059, has both similar shallow C IV BALs and moderate X-ray absorption.

Subject headings: galaxies: active – galaxies: nuclei – X-rays: galaxies – quasars: absorption lines – quasars: individual (CSO 755)

1. INTRODUCTION

Broad absorption line quasars (BALQSOs) are well known to be weak X-ray sources, and their X-ray fluxes cannot be predicted well from their optical brightnesses (e.g., Green & Mathur 1996; Brinkmann et al. 1999; Gallagher et al. 1999; Brandt, Laor, & Wills 2000; Green et al. 2001; Strateva et al. 2005). High-quality *XMM-Newton* and *Chandra* spectra of ≈ 10 BALQSOs obtained during the past five years have shown that their intrinsic column densities are typically $\approx 10^{23} \text{ cm}^{-2}$ (e.g., Gallagher et al. 2002; Chartas et al. 2002, 2003; Grupe et al. 2003). In at least two of these cases, such X-ray spectra have also revealed discrete absorption features suggesting the presence of relativistic outflows (Chartas et al. 2002, 2003); however, the physical connection between the characteristic ultraviolet (UV) and X-ray absorption is not yet clear.

BALQSOs are known to have higher UV–optical polarization on average compared with ‘typical’ quasars, and $\approx 20\%$ of BALQSOs have a continuum polarization level of $\geq 2\%$ (e.g., Hutsemékers, Lamy, & Remy 1998; Schmidt & Hines 1999). The polarization probably arises due to light scattered off an electron or dust ‘mirror’ of moderate optical depth near the center (e.g., Schmidt & Hines 1999), and it

is strongly anti-correlated with the BALQSO detachment index (DI; Weymann et al. 1991), i.e., sources with UV absorption profiles with lower onset velocities show a higher level of UV–optical continuum polarization (e.g., Ogle et al. 1999; Lamy & Hutsemékers 2004). Measurements of the polarization levels of the continuum, broad emission lines, and BAL troughs provide a valuable probe for tracing the inner structure in these sources. Based upon X-ray (*ASCA*) observations of a sample of seven BALQSOs, Gallagher et al. (1999) tentatively suggested that highly polarized BALQSOs (with a level of 2.3%–5% of broad-band optical continuum polarization) may also be the X-ray brightest of that class (see also Brandt et al. 1999). Such a trend could appear, for example, if most of the X-ray light is blocked from direct view by thick material ($\gtrsim 10^{24} \text{ cm}^{-2}$) associated with the BAL flow, and the X-rays we observe are mostly due to scattering. Any connection between UV–optical continuum polarization and X-ray spectral properties would provide an important clue about the geometry of matter in BALQSO nuclei.

Case Stellar Object 755 (hereafter CSO 755; Sanduleak & Pesch 1989; also known as SBS 1524+517 with J2000.0 coordinates: $\alpha = 15:25:53.9$, $\delta = +51:36:49$) is a radio-quiet BALQSO at $z = 2.88$. It is among the most luminous quasars known with $M_B = -28.4$, being the ninth most luminous quasar in the Sloan Digital Sky Survey (SDSS; York et al. 2000) Data Release 3 (Schneider et al. 2005). CSO 755 is most probably a high-ionization BALQSO (HiBAL), since it does not exhibit low-ionization BALs of Al and Fe in the SDSS spectrum, and it is not heavily reddened. A comparison between the UV absorption features in the SDSS spectrum (taken in 2002) and those observed in earlier spectra of the source (e.g., Korista et al. 1993; Glenn, Schmidt, & Foltz 1994; Ogle et al. 1999) suggests that there have been no strong variations in the prop-

¹ Department of Astronomy & Astrophysics, The Pennsylvania State University, University Park, PA 16802, USA; ohad@astro.psu.edu

² Department of Physics & Astronomy, University of California – Los Angeles, Mail Code 154705, 475 Portola Plaza, Los Angeles CA, 90095–4705, USA

³ Dipartimento di Astronomia, Università degli Studi di Bologna, Via Ranzani 1, 40127 Bologna, Italy

⁴ INAF - Osservatorio Astronomico di Bologna, Via Ranzani 1, 40127 Bologna, Italy

⁵ Max-Planck-Institut für extraterrestrische Physik, Postfach 1312, 85741 Garching, Germany

TABLE 1
LOG OF *XMM-Newton* OBSERVATIONS OF CSO 755

Observation Start Date	Net Exposure Time (ks) / Source Counts		
	MOS1	MOS2	pn
2001 December 08	29.0 / 604	29.0 / 584	24.4 / 1920
2001 December 13	14.5 / 334	14.4 / 310	9.7 / 766

erties of the UV absorber. The source is also one of the most optically polarized BALQSOs ($P_V \simeq 3.5\%$), even though its absorption troughs are more detached than those of most high polarization BALQSOs (e.g., Glenn et al. 1994; Ogle 1998; Ogle et al. 1999). Based upon spectropolarimetric observations of the source, Ogle (1998) was able to constrain the angular size of the electron-scattering region to be intermediate between the angular sizes of the high and low velocity BAL clouds in CSO 755. Combining X-ray data with the available UV-optical information on the source may provide further constraints on the geometry and structure of the BAL flow and on the properties of the scattering medium, since the size of the direct X-ray continuum source is expected to be much smaller compared to the sizes of both the UV BALs and the scattering medium responsible for the UV polarization.

The first sensitive X-ray observations of CSO 755 were obtained by *BeppoSAX* in 1999 (Brandt et al. 1999), and it was also tentatively detected by the *ROSAT* All Sky Survey. The *BeppoSAX* observations provided only loose constraints on the X-ray spectral shape of the source and a flux measurement which enabled planning of follow-up X-ray observations. In this paper we present new, high-quality, *XMM-Newton* observations of CSO 755. In § 2 we describe our observations and their reduction, and in § 3 we present the results of the X-ray spectral analysis and variability of the source. In § 4 we discuss our results and the relations between the UV and X-ray properties of CSO 755 as well as those of other BALQSOs from the literature. Throughout the paper we use the standard cosmological model, with parameters $\Omega_\Lambda=0.7$, $\Omega_M=0.3$, and $H_0=70 \text{ km s}^{-1} \text{ Mpc}^{-1}$ (Spergel et al. 2003).

2. OBSERVATIONS AND DATA REDUCTION

We obtained imaging spectroscopic observations of CSO 755 with *XMM-Newton* (Jansen et al. 2001) on 2001 December 8–9 and on 2001 December 13 (hereafter the first and second observations, respectively). The *XMM-Newton* observation log appears in Table 1. The data were processed using standard *SAS*⁶ v6.1.0 and *FTOOLS* tasks. The event files of both observations were filtered to include events with $\text{FLAG}=0$, and $\text{PATTERN}\leq 12$ ($\text{PATTERN}\leq 4$) and $200\leq \text{PI}\leq 12000$ ($150\leq \text{PI}\leq 15000$) for the MOS (pn) detectors. The event files of the first observation were also filtered to remove a ~ 7 ks period of flaring activity at the end of that observation, which was apparent in the light curve of the entire full-frame window. The event files of the second observation were not filtered in time, since more than 90% of the observation was performed during an intense background flaring period with background count rates ~ 15 times higher than nominal values. The exposure times listed in Table 1 reflect the filtered data used in the analysis.

To extract X-ray spectra we used a source-extraction aper-

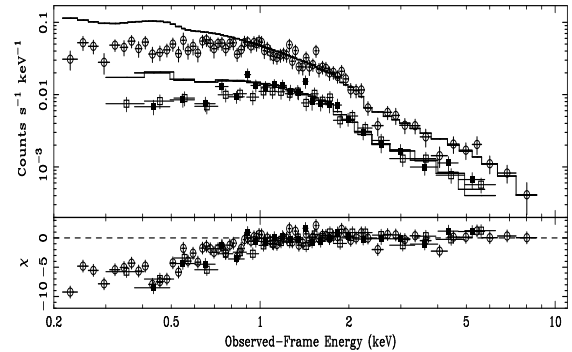


FIG. 1.— Data, best-fit spectra, and residuals for the first *XMM-Newton* observation of CSO 755. Open circles, filled squares, and open squares represent the pn, MOS1, and MOS2 data, respectively. Solid lines represent the best-fit model for each spectrum, and the thick line marks the best-fit model for the pn data. The data were fitted with a Galactic-absorbed power-law in the 5–30 keV rest-frame energy range (~ 1.3 – 7.7 keV in the observed frame), and extrapolated to as low as 0.8 keV in the rest frame. The χ residuals are in units of σ with error bars of size one.

ture radius of $30''$ in the images of all three European Photon Imaging Camera (EPIC) detectors.⁷ Background regions were taken to be at least as large as the source regions; these were annuli (circles) for the MOS (pn) detectors. The redistribution matrix files (RMFs; which include information on the detector gain and energy resolution) and the ancillary response files (ARFs; which include information on the effective area of the instrument, filter transmission, and any additional energy-dependent efficiencies) for the spectra were created with the *SAS* tasks *RMFGEN* and *ARFGEN*, respectively. The spectra were grouped with a minimum of 25 counts per bin using the task *GRPPHA*.

3. X-RAY PROPERTIES OF CSO 755

3.1. Photon Index and Intrinsic Absorption

We used *XSPEC* v11.3.0 (Arnaud 1996) to fit jointly the data from all three EPIC detectors in the first observation with a Galactic-absorbed power law in the rest-frame 5–30 keV energy range (~ 1.3 – 7.7 keV in the observed frame); the Galactic absorption (Dickey & Lockman 1990) was fixed to the value $1.57 \times 10^{20} \text{ cm}^{-2}$ (obtained using the *HEASARC* N_H tool⁸). The fit in the rest-frame 5–30 keV band is acceptable with a derived power-law photon index of $\Gamma=1.94 \pm 0.12$. However, extrapolation of this model to lower rest-frame energies reveals strong negative residuals; these indicate the presence of intrinsic X-ray absorption (Fig. 1). We therefore added an intrinsic (redshifted) neutral absorption component with solar abundances to the model and fitted the data of each EPIC detector alone, jointly fitted the data of the two MOS detectors, and jointly fitted all three EPIC detectors. The best-fit results of this model for the two observations are summarized in Table 2. The best-fit spectral parameters for all three EPIC detectors are consistent within the errors. The EPIC spectra from the first observation and their joint, best-fit model appear in Fig. 2, which also includes a confidence-contour plot of the Γ – N_H parameter space.

The $\sim 2\sigma$ residuals apparent in Fig. 2 at observed-frame energies $\lesssim 0.4$ keV, may be due to a combination of calibration

⁷ The two Reflection Grating Spectrometer detectors on *XMM-Newton* do not have sufficient counts to perform a high-resolution spectral analysis for CSO 755.

⁸ <http://heasarc.gsfc.nasa.gov/cgi-bin/Tools/w3nh/w3nh.pl>

⁶ *XMM-Newton* Science Analysis System. See http://xmm.vilspa.esa.es/external/xmm_sw_cal/sas_frame.shtml

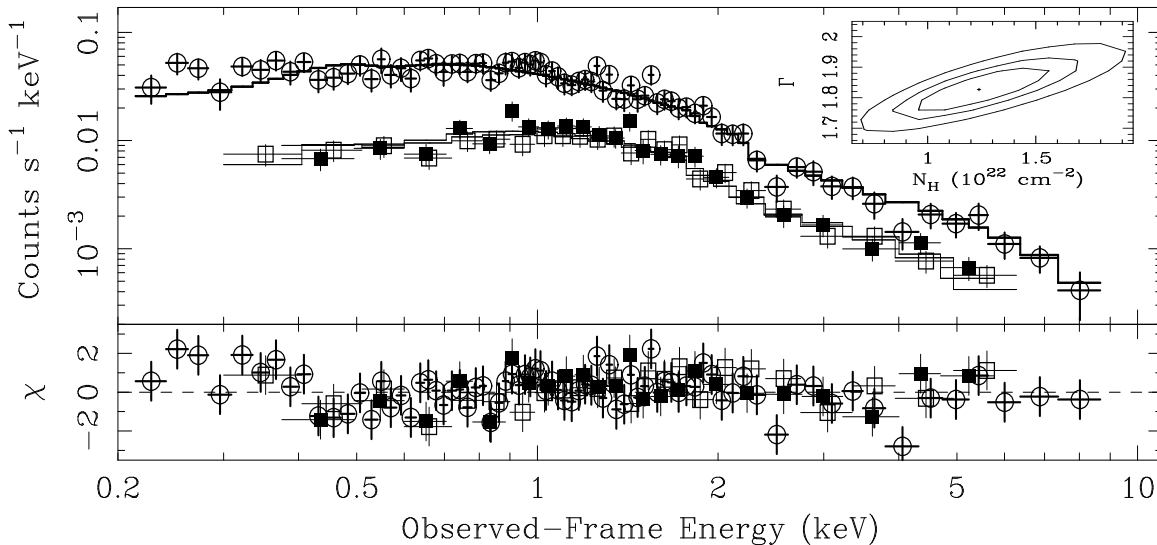


FIG. 2.— Data, best-fit spectra, and residuals for the first *XMM-Newton* observation of CSO 755. Symbols are the same as those of Fig. 1. The χ residuals are in units of σ with error bars of size one. The inset shows 68, 90, and 99% confidence contours for the intrinsic absorption (N_{H}) and photon index (Γ).

uncertainties (e.g., Sembay et al. 2004; Kirsch et al. 2004) and intrinsic absorption that is somewhat more complex than the simple neutral-absorption model we have applied (perhaps due to the partial covering, ionization, or internal velocity structure of the absorber). To investigate the nature of these residuals and to check whether some of the absorption could be due to ionized gas, we fit the data with a model consisting of a Galactic-absorbed power-law and an ionized absorber using the XSPEC model ABSORI (Done et al. 1992; Magdziarz & Zdziarski 1995). We found a photon index of 1.99 ± 0.10 , and an ionized column density of $N_{\text{H}} = 1.0 \pm 0.3 \times 10^{23} \text{ cm}^{-2}$. At face value, an F -test showed that this model provided a better fit to the data over the model that used a neutral intrinsic absorber [$\chi^2(\text{DOF}) = 85.2(120)$ for jointly fitting the three EPIC detectors; compare with Table 2], and the best-fit spectrum showed that the $\sim 2\sigma$ residuals observed at $\lesssim 0.4$ keV have almost disappeared. However, the use of an ionized absorber model in our case is almost certainly a simplistic approach to a more complex problem of BAL flows. More detailed modeling of AGN outflows has been performed for several moderate-luminosity sources (e.g., Netzer et al. 2003; Chelouche & Netzer 2005), but appropriate models have not yet been developed for luminous BALQSOs. Moreover, due to the high redshift of CSO 755, $z = 2.88$, any modeling is highly influenced by the low observed-frame energy bins at the edge of the EPIC response ($\lesssim 0.4$ keV). Any fitting carried out in this energy range depends on a handful of data points, and is somewhat unreliable due to the calibration uncertainties discussed above.

When fit with a neutral-absorption model, CSO 755 has a relatively low X-ray column density of $N_{\text{H}} = 1.2 \pm 0.3 \times 10^{22} \text{ cm}^{-2}$ (Table 2 and Fig. 2), compared to other BALQSOs ($N_{\text{H}} \sim 10^{23} \text{ cm}^{-2}$) fit with the same model (e.g., Gallagher et al. 2002). The power-law photon index in the rest-frame ~ 0.8 –30 keV band, $\Gamma = 1.83^{+0.07}_{-0.06}$, is well within the typical range of indices for other BALQSOs (Gallagher et al. 2002) and, in fact, is within the range for all radio-quiet type 1 (i.e., unobscured) AGNs (e.g., Reeves & Turner 2000; Shemmer et al. 2005; Vignali et al. 2005). This supports the conclusion that intrinsic BALQSO X-ray

continua are not different from those of ‘typical’ radio-quiet type 1 AGNs (e.g., Gallagher et al. 2002).

The analyses performed throughout the rest of this paper are based upon the data of all three EPIC detectors from the first observation. The data from the second observation, which were not filtered in time, exhibit poor signal-to-noise ratios which result in large uncertainties on the best-fit parameters (although these results are generally in agreement with those based upon the data from the first observation; see Table 2).

3.2. Iron Features and Compton Reflection

The EPIC data show a hint of the presence of an iron absorption edge in the rest-frame energy range 7.1–9.3 keV, where the low-energy end of this range corresponds to the threshold energy of Fe I, and the high-energy end corresponds to the threshold energy of Fe XXVI (Verner et al. 1993). In order to test for the existence of an iron edge we fit a model consisting of a Galactic-absorbed power law, a neutral intrinsic absorption component, and an iron-edge component (the EPIC spectral resolution should, in principle, allow us to resolve such an edge). We fitted the data with this model first using a neutral edge, and then fitted an ionized edge. The threshold of the neutral edge was fixed at a rest-frame energy of 7.1 keV, and the threshold of the ionized edge was fixed at rest-frame 9.3 keV; the strength of the edge was free to vary. Using an F -test we found that the model using a neutral iron edge did not significantly improve the fit over the model we used in § 3.1, and the upper limit we obtained on the absorption depth of a neutral edge is $\tau \leq 0.1$. Fitting the data with an ionized iron edge significantly improves the fit from § 3.1; we obtained a $\chi^2(\text{DOF}) = 102.1(120)$, compared with the $\chi^2(\text{DOF}) = 107.6(121)$ obtained using the model of § 3.1 (see also Table 2). The absorption depth of an ionized edge is $\tau = 0.4^{+0.2}_{-0.3}$. However, the suggested ionized iron edge, at an observed energy of ~ 2.4 keV, coincides with the pronounced Au M edge in the EPIC spectral response, leading to some uncertainty about its existence.

Some BALQSOs have shown evidence for X-ray ‘reflection’ via either Fe $K\alpha$ lines or Compton-reflection ‘humps’ (e.g., Oshima et al. 2001; Gallagher et al. 2002; Turner &

TABLE 2
BEST-FIT X-RAY SPECTRAL PARAMETERS FOR CSO 755.

Detector	2001 December 8			2001 December 13		
	N_{H}^{a}	Γ	$\chi^2(\text{DOF})$	N_{H}^{a}	Γ	$\chi^2(\text{DOF})$
PN	$1.17^{+0.37}_{-0.35}$	$1.86^{+0.09}_{-0.09}$	68.7(75)	$1.85^{+2.17}_{-1.41}$	$1.70^{+0.49}_{-0.18}$	135.9(122)
MOS1	$2.40^{+1.21}_{-0.99}$	$1.92^{+0.18}_{-0.17}$	16.2(21)	≤ 1.43	$1.80^{+0.39}_{-0.27}$	18.3(31)
MOS2	$1.07^{+0.87}_{-0.75}$	$1.71^{+0.17}_{-0.15}$	14.6(21)	≤ 1.86	$1.71^{+0.44}_{-0.33}$	16.5(28)
MOS1+MOS2	$1.67^{+0.71}_{-0.63}$	$1.81^{+0.12}_{-0.12}$	33.2(44)	≤ 1.20	$1.76^{+0.27}_{-0.23}$	35.2(61)
MOS1+MOS2+PN	$1.24^{+0.31}_{-0.31}$	$1.83^{+0.07}_{-0.06}$	107.6(121)	$0.89^{+0.83}_{-0.71}$	$1.74^{+0.24}_{-0.21}$	177.6(185)

NOTE. — The best-fit intrinsic absorption (N_{H}), photon index (Γ), normalization, and χ^2 were obtained from a model consisting of a power law with both Galactic and neutral intrinsic absorption. The lack of low-energy response and low signal-to-noise ratio make MOS detector data less sensitive for constraining N_{H} in the second observation.

^aIntrinsic column density in units of 10^{22} cm^{-2} . Errors are calculated taking one parameter to be of interest ($\Delta\chi^2 = 2.71$; e.g., Avni 1976).

Kraemer 2003; Chartas et al. 2004; Gallagher et al. 2005). The Compton-reflection ‘hump’ is the spectral manifestation of hard X-ray photons emitted in a corona of hot electrons and reflected off the relatively colder accretion disk (e.g., see § 3.5 of Reynolds & Nowak 2003 and references therein). The Compton-reflection ‘hump’ feature lies in the rest-frame ~ 7 –60 keV energy range, peaking at rest-frame ~ 30 keV. Both the Fe $K\alpha$ line and Compton reflection spectral components are expected to be prominent if most of the observed X-ray flux from the source is reflected or scattered. No clear sign of either a neutral (at rest-frame 6.4 keV) or an ionized (at rest-frame 6.7–6.97 keV) Fe $K\alpha$ emission line, or any sign of a Compton-reflection component, is apparent in the EPIC spectra of CSO 755.

To constrain the strengths of Fe $K\alpha$ lines and the Compton ‘hump’ we used XSPEC to fit the spectra with two models. The first model contained a power-law with Galactic and intrinsic absorption, a Compton-reflection component of X-rays reflected off a neutral disk (using the PEXRAV model; Magdziarz & Zdziarski 1995), and a neutral narrow Gaussian Fe $K\alpha$ line that had a fixed width of $\sigma=0.1$ keV and a fixed rest-frame energy of 6.4 keV during the fit. The second model contained a power-law with Galactic and intrinsic absorption, a Compton-reflection component of X-rays reflected off an ionized disk (using the PEXRIV model; Magdziarz & Zdziarski 1995), and an ionized narrow Gaussian Fe $K\alpha$ line that had a fixed width of $\sigma=0.1$ keV and a fixed rest-frame energy of 6.7 keV during the fit. The photon indices and intrinsic absorption columns in the two fits were not significantly different than the ones obtained in § 3.1. We obtained upper limits (90% confidence) on the rest-frame equivalent width of a neutral Fe $K\alpha$ line of 180 eV, and on the rest-frame equivalent width of an ionized Fe $K\alpha$ line of 120 eV. Similarly, we obtained an upper limit on the relative Compton-reflection parameter of X-rays reflected off a neutral disk, $R \leq 0.2$. For the PEXRIV model we obtained a relative Compton-reflection parameter off an ionized disk of $R=1.1^{+1.5}_{-0.8}$. However, an F -test indicates that the existence of this component is not warranted by the data, and that the marginal improvement in the fit [$\chi^2(\text{DOF})=99.6(118)$], relative to the fit of § 3.1 (Table 2), is probably due to the ionized iron edge which is in-

cluded in the PEXRIV model; the significance of this edge’s existence was already investigated above. Motivated by recent claims of relativistic broad absorption lines in the X-ray spectra of some BALQSOs (e.g., Chartas et al. 2002, 2003), we searched for additional absorption features in the X-ray spectrum of CSO 755, but our spectrum is featureless.

3.3. X-ray ‘Loudness’

Using the SDSS spectrum of CSO 755 we computed the optical-to-X-ray spectral energy distribution (SED) parameter (or X-ray ‘loudness’ parameter), α_{ox} , defined as:

$$\alpha_{\text{ox}} = \frac{\log(f_{2 \text{ keV}}/f_{2500 \text{ \AA}})}{\log(\nu_{2 \text{ keV}}/\nu_{2500 \text{ \AA}})} \quad (1)$$

where $f_{2 \text{ keV}}$ and $f_{2500 \text{ \AA}}$ are the monochromatic fluxes at rest-frame 2 keV and 2500 Å, respectively (e.g., Tananbaum et al. 1979). We estimated the monochromatic flux at rest-frame 2500 Å by extrapolating the monochromatic flux at rest-frame 1350 Å assuming a continuum of the form $f_{\nu} \propto \nu^{-\alpha}$ with $\alpha = 0.5$ (Vanden Berk et al. 2001). This continuum slope is consistent with the one we measured from the SDSS spectrum ($\alpha \approx 0.4 - 0.6$) that shows no indication for intrinsic reddening. The monochromatic flux at rest-frame 2 keV was computed using the power-law normalization at 1 keV of the pn detector, $4.5 \times 10^{-5} \text{ keV cm}^{-2} \text{ s}^{-1} \text{ keV}^{-1}$, and the spectral parameters of the joint fit of all EPIC detectors in the first observation (Table 2). We find an observed (i.e., corrected for Galactic absorption, but *not* corrected for intrinsic absorption) $\alpha_{\text{ox}}=-1.54$. When correcting for intrinsic absorption we find $\alpha_{\text{ox}}=-1.51$, which is consistent with the mean absorption-corrected value, $\alpha_{\text{ox}}=-1.58$, for a non-uniform sample of seven BALQSOs, for which α_{ox} could be measured from high-quality X-ray observations (Gallagher et al. 2002). Note that the intrinsic-absorption correction to α_{ox} for CSO 755 is relatively small owing to its small X-ray absorption column density (see § 3.1). Given the large optical luminosity of CSO 755, the α_{ox} we find is also consistent with $\alpha_{\text{ox}}=-1.73$ expected for the source by the relationship between α_{ox} and the monochromatic luminosity at 2500 Å (Eq. 6 of Strateva et al. 2005). Although the difference between $\alpha_{\text{ox}}=-1.51$

and $\alpha_{\text{ox}} = -1.73$ corresponds to a difference of ~ 3.7 in X-ray flux (Eq. 1), this is within the scatter around the Strateva et al. (2005) relation. In fact, CSO 755 was selected for the *XMM-Newton* observations as being one of the most X-ray luminous quasars, and hence its relatively high (i.e., less negative) α_{ox} ; using our first observation, correcting for Galactic absorption and for the best-fit neutral intrinsic absorption we found in § 3.1, we measure $L_{2-10 \text{ keV}} = 8.4 \times 10^{45} \text{ ergs s}^{-1}$. This luminosity exceeds the 2–10 keV luminosities of the ten sources in the Shemmer et al. (2005) study, and is exceeded by only one source from the Vignali et al. (2005) study; the sources in those two studies are among the most X-ray luminous known.

3.4. X-ray Variability

Motivated by the recent discovery of pronounced X-ray variations in the BALQSO PG 2112+059 (Gallagher et al. 2004b), we tested whether CSO 755 exhibits long or short-term X-ray flux variations. Brandt et al. (1999) report a 2–10 keV flux of $1.3 \times 10^{-13} \text{ ergs cm}^{-2} \text{ s}^{-1}$ for the *BepoSAX* observations of the source. For our first observation we find a 2–10 keV flux of $(1.50_{-0.16}^{+0.14}) \times 10^{-13} \text{ ergs cm}^{-2} \text{ s}^{-1}$ for the EPIC pn detector (90% confidence). Similarly, we find a 2–10 keV flux of $(1.58_{-0.56}^{+0.70}) \times 10^{-13} \text{ ergs cm}^{-2} \text{ s}^{-1}$ for the EPIC pn detector in our second observation. These three flux measurements were made in the 2–10 keV observed-frame energy range, and were not corrected for either Galactic or intrinsic absorption. We also compared the total count rates above the background level for each EPIC detector in each of our two *XMM-Newton* observations. The results are consistent with the flux measurements, i.e., $\lesssim 10\%$ flux variations within a rest-frame timescale of $\sim 1 \text{ d}$ (see Table 1). The fluxes we measure in the two *XMM-Newton* observations are also consistent with the *BepoSAX* measurement, given the relative uncertainty between cross-calibrations of the two observatories (e.g., Kirsch et al. 2004), suggesting that flux variations may be $\lesssim 10\%$ even on a $\sim 1 \text{ yr}$ rest-frame timescale (although there is scope for variability in between those two epochs). Using PIMMS⁹, we found that the X-ray flux of CSO 755 obtained from the tentative *ROSAT* detection is also consistent with the fluxes measured from the *BepoSAX* and *XMM-Newton* observations. We note that a 10 ks *XMM-Newton* guaranteed time observation of CSO 755, carried out on 2001 July 30, does not allow a meaningful flux measurement for variability purposes, since the entire observation is ruined by high background flaring. Finally, we searched for rapid ($\sim 1 \text{ hr}$ timescale in the rest frame) variability within our first *XMM-Newton* observation applying a Kolmogorov-Smirnov test to the photon arrival times, but none was detected. We also created a light curve for that observation, binning the photon arrival times in bins of 100 s; the excess variance (e.g., Nandra et al. 1997) was consistent with zero.

4. DISCUSSION

4.1. X-ray Spectrum

Our *XMM-Newton* spectrum of CSO 755 is among the three highest signal-to-noise X-ray spectra of BALQSOs to date (see Chartas et al. 2002, 2003; Table 1). The photon index $\Gamma = 1.83_{-0.06}^{+0.07}$ and the absorption-corrected

optical-to-X-ray spectral slope $\alpha_{\text{ox}} = -1.51$ show that this source has an X-ray continuum of a ‘typical’ radio-quiet quasar (e.g., Vignali et al. 2005). Our results are therefore in line with the conclusion that the X-ray continua of BALQSOs are not intrinsically different from those of the majority of the quasar population.

We find that the X-ray spectrum of CSO 755 is moderately absorbed, with hints of a complex absorption pattern at rest-frame energies $\lesssim 1.5 \text{ keV}$. The best-fit neutral intrinsic column density is $N_{\text{H}} \sim 1.2 \times 10^{22} \text{ cm}^{-2}$, and our data do not allow us to rule out the possibility that there is some absorption by ionized gas, with column densities of $\approx 10^{23} \text{ cm}^{-2}$. Even though we cannot rule out the possibility that there are other X-ray components in the source which are much more absorbed, the $\alpha_{\text{ox}} = -1.51$ we obtain is already quite flat (i.e., more X-ray bright) relative to the α_{ox} found in radio-quiet quasars with similar luminosities. Any additional absorption would have required the intrinsic α_{ox} to be even flatter, which is unlikely. Even though the redshift of CSO 755 gives us a good opportunity to measure the high-energy iron features with *XMM-Newton* to respectable accuracy, we did not detect any features, such as the relativistic broad Fe absorption lines perhaps observed in the BALQSOs APM 08279+5255 (Chartas et al. 2002) and PG 1115+080 (Chartas et al. 2003). The only X-ray manifestation of the UV absorber in CSO 755 therefore lies in the relatively low intrinsic neutral column we detect at low energies. Our results bolster the idea that BALQSOs display a range of intrinsic columns ($\approx 10^{22} - 10^{24} \text{ cm}^{-2}$), and a broad range of X-ray spectral features.

The absence of prominent iron lines or a Compton-reflection ‘hump’ in the spectrum of CSO 755 indicates that X-ray reflection from the disk into our line-of-sight is weak or absent. The idea that most of the X-rays are directly observed is also indicated by the rather flat α_{ox} we find. Since most of the X-rays are directly observed, and are not scattered or reflected, one might have expected the source to exhibit some level of X-ray flux variations. However, we do not detect significant variability on either short ($\lesssim 1 \text{ d}$) or long ($\sim 1 \text{ yr}$) timescales. This may be an indicator of a large black-hole mass, $M_{\text{BH}} \gtrsim 10^9 M_{\odot}$, in the source (e.g., O’Neill et al. 2005). In fact, assuming Eddington-limited accretion, we estimate a black hole mass of $M_{\text{BH}} \gtrsim 5 \times 10^9 M_{\odot}$ from the optical luminosity of the source.

4.2. UV–Optical Polarization and X-ray Properties

Based upon the relatively high UV–optical polarization level of CSO 755 ($P_V \simeq 3.5\%$), it might have been possible for most of the observed X-ray flux from the source to be scattered or reflected. The fact that the bulk of the X-ray emission from CSO 755 appears to be directly observed, however, calls for an investigation of the relationship between UV–optical polarization and X-ray properties in a larger sample of BALQSOs. We have compiled a non-uniform sample of 46 BALQSOs from the literature (including the CSO 755 data presented in this paper) which have published X-ray properties (Gallagher et al. 2002; Grupe et al. 2003; Gallagher et al. 2004a; Gallagher et al. in prep.) and corresponding UV–optical polarization measurements (Hutsemékers et al. 1998; Ogle et al. 1999; Schmidt & Hines 1999; Hutsemékers & Lamy 2000, 2001). We have not found significant correlations between the broad-band UV–optical polarization level and any of the following X-ray properties: α_{ox} , hardness ratio, photon index, neutral intrinsic absorption, flux, and luminosity. In particular, the suggestion that highly polarized BALQSOs are also

⁹ Portable Interactive Multi-Mission Simulator at <http://heasarc.gsfc.nasa.gov/Tools/w3pimms.html>

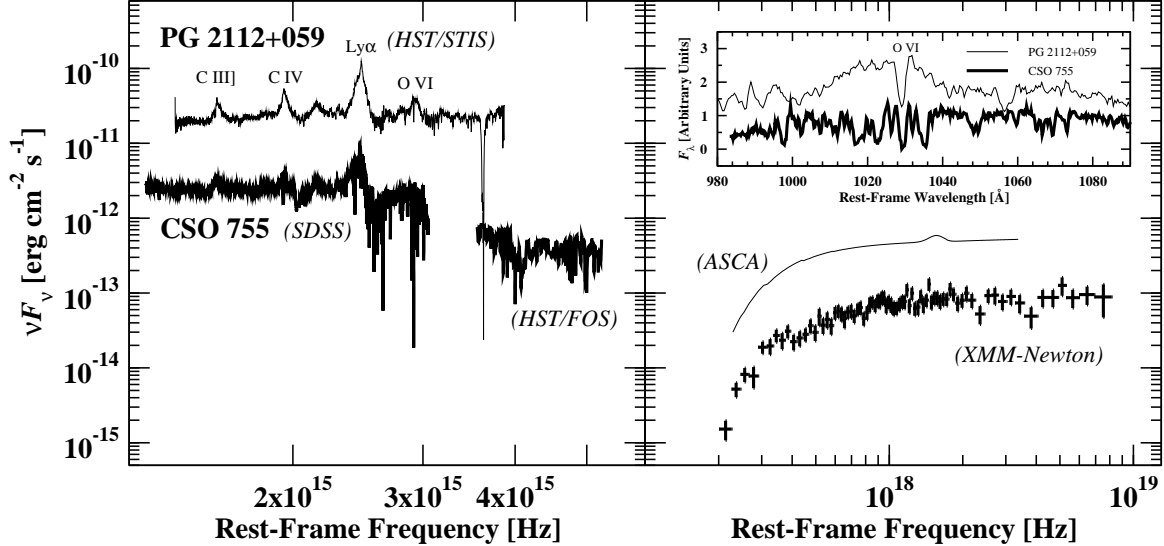


FIG. 3.— The observed SED of CSO 755 (*thick lines*) plotted along with the observed SED of PG 2112+059 (*thin lines*). For clarity, only the X-ray observations of the first epoch (ASCA) are shown for PG 2112+059 (see Gallagher et al. 2004b). All the SEDs are dereddened to remove Galactic absorption. The insert shows the O VI λ 1034 region of the two sources. Note the remarkable similarity between the UV–X-ray SEDs of the two sources.

the X-ray brightest (or more X-ray luminous) is not supported by our analysis (Gallagher et al. 1999). We caution, however, that the UV–optical polarization data are not homogeneous, and are subject to considerable measurement uncertainties.

4.3. Comparison with the BALQSO PG 2112+059

Some of the UV–X-ray properties of CSO 755 are similar to those of the well-studied BALQSO PG 2112+059 (Gallagher et al. 2001, 2004b). For example, both sources display shallow BAL troughs in the UV, and their neutral intrinsic column densities, $N_{\text{H}} \sim 10^{22} \text{ cm}^{-2}$, are among the lowest columns observed in BALQSOs. It is therefore possible that shallow BAL troughs are associated with relatively mild X-ray absorption; we are not aware of any counterexamples. To test this possibility, high-quality X-ray observations of more BALQSOs with shallow troughs are required.

In Fig. 3 we plot the observed SED of CSO 755 along with that of PG 2112+059. The SEDs have been corrected for Galactic absorption. One can see that the general shapes of the UV spectra of the two sources are quite similar to one another, and that a remarkable similarity is apparent between the ASCA spectrum of PG 2112+059 and our XMM-Newton spectrum of CSO 755. In fact, scaling down the ASCA model for PG 2112+059 by a factor of ~ 6 in flux makes it almost identical to our XMM-Newton spectrum of CSO 755. The UV spectrum of CSO 755 is scaled down by an almost constant factor of ~ 10 in flux relative to the UV spectrum of PG 2112+059. The difference between the X-ray and UV scaling factors is also consistent with the difference in α_{ox} of the two sources (see § 3.3; Gallagher et al. 2004b). The main differences between the two sources lie in the details of their UV spectra, which are apparent in the insert to Fig. 3, and the fact that in contrast with CSO 755, PG 2112+059 is a low-polarization BALQSO, though polarization data for this source are not available in the literature covering the same rest-frame wavelengths as for CSO 755. In addition, as opposed to PG 2112+059, CSO 755 did not show any X-ray variations.

5. SUMMARY

We have presented new XMM-Newton observations of CSO 755 that provide one of the best BALQSO X-ray spectra. Our main results can be summarized as follows:

1. The power-law X-ray photon index we found, $\Gamma = 1.83^{+0.07}_{-0.06}$, is consistent with photon indices observed for ‘typical’ radio-quiet quasars.
2. The intrinsic $\alpha_{\text{ox}} = -1.51$ we found is rather flat (X-ray bright) but is consistent with the α_{ox} distribution observed for radio-quiet quasars of similar luminosity.
3. By fitting the spectrum with a neutral-absorption model, we found a column density of $N_{\text{H}} \sim 1.2 \times 10^{22} \text{ cm}^{-2}$, which is among the lowest X-ray columns measured for BALQSOs.
4. We did not detect, with high significance, any other emission or absorption features in the X-ray spectrum. The lack of signatures of either an Fe K α line or a Compton-reflection component suggests that most of the X-rays from the source are directly observed rather than being scattered or reflected, as might have been expected given the source’s high level of UV–optical polarization; this is also supported by the relatively flat intrinsic α_{ox} we measured.
5. We found that the UV–optical continuum polarization level of BALQSOs is not correlated with any of their X-ray properties, based on a sample of 46 BALQSOs from the literature, including CSO 755.
6. A lack of significant short- and long-term X-ray flux variations in CSO 755 may be attributed to a large black-hole mass in the source.
7. We note that both CSO 755 and another luminous BALQSO, PG 2112+059, display both shallow C IV BAL troughs and moderate X-ray absorption, suggesting a possible relationship between these two properties.

This work is based on observations obtained with *XMM-Newton*, an ESA science mission with instruments and contributions directly funded by ESA Member States and the USA (NASA). We gratefully acknowledge the financial support of NASA grant NAG5-9932 (OS, WNB), NASA LTSA grant NAG5-13035 (WNB), and MIUR COFIN

grant 03-02-23 (AC, CV). Support for SCG was provided by NASA through the *Spitzer* Fellowship Program, under award 1256317. We are grateful to Shai Kaspi and Doron Chelouche for useful discussions. We also appreciate the constructive comments made by the referee, Mike Brotherton, that helped to improve the manuscript.

REFERENCES

- Arnaud, K. A. 1996, ASP Conf. Ser. 101: Astronomical Data Analysis Software and Systems V, 101, 17
- Avni, Y. 1976, ApJ, 210, 642
- Brandt, W. N., Comastri, A., Gallagher, S. C., Sambruna, R. M., Boller, T., & Laor, A. 1999, ApJ, 525, L69
- Brandt, W. N., Laor, A., & Wills, B. J. 2000, ApJ, 528, 637
- Brinkmann, W., Wang, T., Matsuoka, M., & Yuan, W. 1999, A&A, 345, 43
- Chartas, G., Brandt, W. N., Gallagher, S. C., & Garmire, G. P. 2002, ApJ, 579, 169
- Chartas, G., Brandt, W. N., & Gallagher, S. C. 2003, ApJ, 595, 85
- Chartas, G., Eracleous, M., Agol, E., & Gallagher, S. C. 2004, ApJ, 606, 78
- Chelouche, D., & Netzer, H. 2005, ApJ, 625, 95
- Dickey, J. M., & Lockman, F. J. 1990, ARA&A, 28, 215
- Done, C., Mulchaey, J. S., Mushotzky, R. F., & Arnaud, K. A. 1992, ApJ, 395, 275
- Gallagher, S. C., Brandt, W. N., Sambruna, R. M., Mathur, S., & Yamasaki, N. 1999, ApJ, 519, 549
- Gallagher, S. C., Brandt, W. N., Laor, A., Elvis, M., Mathur, S., Wills, B. J., & Iyomoto, N. 2001, ApJ, 546, 795
- Gallagher, S. C., Brandt, W. N., Chartas, G., & Garmire, G. P. 2002, ApJ, 567, 37
- Gallagher, S. C., Brandt, W. N., Chartas, G., Garmire, G. P., & Sambruna, R. M. 2004a, Advances in Space Research, 34, 2594
- Gallagher, S. C., Brandt, W. N., Wills, B. J., Charlton, J. C., Chartas, G., & Laor, A. 2004b, ApJ, 603, 425
- Gallagher, S. C., et al. 2005, ApJ, in press (astro-ph/0506616)
- Glenn, J., Schmidt, G. D., & Foltz, C. B. 1994, ApJ, 434, L47
- Green, P. J., & Mathur, S. 1996, ApJ, 462, 637
- Green, P. J., Aldcroft, T. L., Mathur, S., Wilkes, B. J., & Elvis, M. 2001, ApJ, 558, 109
- Grupe, D., Mathur, S., & Elvis, M. 2003, AJ, 126, 1159
- Hutsemekers, D., Lamy, H., & Remy, M. 1998, A&A, 340, 371
- Hutsemekers, D., & Lamy, H. 2000, A&A, 358, 835
- Hutsemekers, D., & Lamy, H. 2001, A&A, 367, 381
- Jansen, F., et al. 2001, A&A, 365, L1
- Kirsch, M. G. F., et al. 2004, Proc. SPIE, 5488, 103
- Korista, K. T., Voit, G. M., Morris, S. L., & Weymann, R. J. 1993, ApJS, 88, 357
- Lamy, H., & Hutsemekers, D. 2004, A&A, 427, 107
- Magdziarz, P., & Zdziarski, A. A. 1995, MNRAS, 273, 837
- Nandra, K., George, I. M., Mushotzky, R. F., Turner, T. J., & Yaqoob, T. 1997, ApJ, 476, 70
- Netzer, H., et al. 2003, ApJ, 599, 933
- Ogle, P. M. 1998, Ph.D. Thesis
- Ogle, P. M., Cohen, M. H., Miller, J. S., Tran, H. D., Goodrich, R. W., & Martel, A. R. 1999, ApJS, 125, 1
- O'Neill, P. M., Nandra, K., Papadakis, I. E., & Turner, T. J. 2005, MNRAS, 358, 1405
- Oshima, T., et al. 2001, ApJ, 563, L103
- Reeves, J. N., & Turner, M. J. L. 2000, MNRAS, 316, 234
- Reynolds, C. S., & Nowak, M. A. 2003, Phys. Rep., 377, 389
- Sanduleak, N., & Pesch, P. 1989, ApJS, 70, 173
- Schmidt, G. D., & Hines, D. C. 1999, ApJ, 512, 125
- Schneider, D. P., et al. 2005, AJ, 130, 367
- Sembay, S., et al. 2004, Proc. SPIE, 5488, 264
- Shemmer, O., Brandt, W. N., Vignali, C., Schneider, D. P., Fan, X., Richards, G. T., & Strauss, M. A. 2005, ApJ, 630, 729
- Spergel, D. N., et al. 2003, ApJS, 148, 175
- Strateva, I. V., Brandt, W. N., Schneider, D. P., Vanden Berk, D. G., & Vignali, C. 2005, AJ, 130, 387
- Tananbaum, H., et al. 1979, ApJ, 234, L9
- Turner, T. J., & Kraemer, S. B. 2003, ApJ, 598, 916
- Vanden Berk, D. E., et al. 2001, AJ, 122, 549
- Verner, D. A., Yakovlev, D. G., Band, I. M., & Trzhaskovskaya, M. B. 1993, Atomic Data and Nuclear Data Tables, 55, 233
- Vignali, C., Brandt, W. N., Schneider, D. P., & Kaspi, S. 2005, AJ, 129, 2519
- Weymann, R. J., Morris, S. L., Foltz, C. B., & Hewett, P. C. 1991, ApJ, 373, 23
- York, D. G., et al. 2000, AJ, 120, 1579